Available online at www.sciencedirect.com
SCIENCE DIRECT
Journal of Non-Crystalline Solids 352 (2006) 1765–1768
JOURNAL OF NON-CRYSTALLINE SOLIDS
www.elsevier.com/locate/jnoncrysol

# Analysis of electrical characteristics of high performance pentacene thin-film transistors with PMMA buffer layer

F. De Angelis, L. Mariucci *, S. Cipolloni, G. Fortunato

*IFN-CNR, via Cineto Romano 42, 00156 Roma, Italy*

Available online 27 March 2006

**Abstract**

Top contact and bottom contact TFTs, based on evaporated pentacene, have been fabricated by using PMMA as buffer layer. Both type of devices show high performance with field-effect mobility >1 $cm^2/V$ s. Top contact transfer characteristics, measured at different temperatures, have been analyzed by the 'temperature method' in order to evaluate the effective density of localized states (DOS). The calculated DOS, approximated by two exponential tails, has been used in 2D numerical device analysis program to simulate the transfer and output characteristics at different temperatures.


*PACS:* 72.80.Le; 85.30.De; 85.30.Tv

*Keywords:* Thin-film transistors; Band structure; Conductivity; Polymers and organics

## 1. Introduction

The new opportunities that the use of organic semiconductors offer to device fabrication in the field of large area, low-cost and flexible electronics, have recently increased the research efforts on these materials [1]. Recent results have shown that devices based on some organic semiconductor can be easily compared with those based amorphous silicon [2]. Indeed, the performance obtained with pentacene-based organic thin-film transistors (OTFTs) [2] make possible that OTFTs are used as drivers of organic light emitting diodes (OLEDs) in high-resolution active matrix displays.

To optimize the device characteristics of OTFTs it is very important to understand the transport mechanisms. In fact, many problems related to the understanding of the transport phenomena [3,4] and the aging effects of the organic semiconductors [4,5] are still open.

In this work we analyze the electrical characteristics, measured at different temperatures, of high quality polycrystalline pentacene-TFTs, obtained by using polymethylmetacrylate (PMMA) as buffer layer [6,7]. From the field-effect analysis of the electrical characteristics we determined the effective density of localized states of the active pentacene layer.

## 2. Experimental

Devices have been fabricated on heavily doped silicon wafers, acting as gate electrode, thermally oxidized to form the gate dielectric (silicon dioxide thickness of $d_{ox} = 150$ and 60 nm). In bottom contact (BC) configuration the source and drain gold contacts (30 nm thick) have been defined by optical lithography and wet etching with channel lengths $L = 7$, 15, 25, 100, 500 μm and channel width $W = 200$ μm. Before pentacene deposition, the samples have been spin coated with a film of PMMA 950 K (about 8 nm thick) annealed at 90 °C for 10 min. It has been shown that thin PMMA films can been used as buffer layer in order to improve the quality of the polycrystalline pentacene [6,7]. Thermal evaporation of pentacene (Sigma

* Corresponding author. Tel.: +39 641522229; fax: +39 641522220.
*E-mail addresses:* mariucci@ifn.cnr.it, luigi.mariucci@ifn.cnr.it (L. Mariucci).

0022-3093/$ - see front matter © 2006 Elsevier B.V. All rights reserved.
doi:10.1016/j.jnoncrysol.2005.11.123

Aldrich, 97% purity) has been performed on the samples without extra purification process or substrate heating (evaporation rate about 3 nm/min). For top contact (TC) configuration, source/drain gold contacts are evaporated through a shadow mask on top of pentacene active layer ($L = 100$ μm, $W = 200$ μm).

## 3. Results and discussion

Transfer characteristics of both top and bottom configurations, measured at $V_{ds} = -1$ V, are shown in Fig. 1. TC devices exhibit field-effect mobility $\mu_{FE} = 1.4$ cm$^2$/V s, subthreshold slope, measured at the onset of subthreshold region, $S = 0.5$ V/dec, threshold voltage $V_{th} = -13.5$ V, whereas BC devices, with $L = 100$ μm, show $\mu_{FE} = 1.1$ cm$^2$/V s, $S = 0.3$ V/dec, and $V_{th} = -6.6$ V. We note that BC devices presented in this work show among the best performance reported for long-channel pentacene-based TFTs in BC configuration [8,9]. The output characteristics of TC and BC devices (see Fig. 2) show a good linear behavior at low $V_{ds}$ as well as an excellent saturation region at high $V_{ds}$. The observed difference between TC and BC electrical characteristics could be related to the different device structure [7]: while in TC device the current flows from the channel to the drain through the pentacene active layer in the BC configuration holes are injected from the gold source contact into the pentacene channel through the PMMA buffer layer and are extracted from the drain also through the PMMA. The parasitic resistance introduced by the buffer layer reduces the $\mu_{FE}$ in BC devices with shorter channel lengths and $\mu_{FE} = 0.37$ cm$^2$/V s has been obtained for $L = 7$ μm. However, the linear behavior of the output characteristics of short channel BC TFTs at low drain voltage suggests that the thin PMMA buffer layer still allows sufficiently good ohmic contacts.

Transfer characteristics of TC pentacene TFTs have been measured at different temperatures in the range between 200 K and 320 K (see Fig. 3). As shown in Fig. 4, field-effect mobility and threshold voltage, evaluated

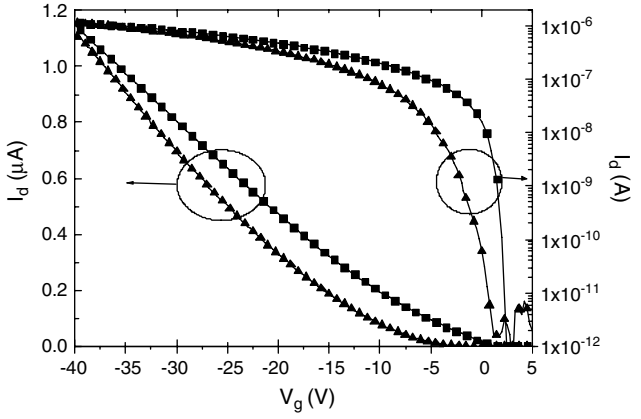


Fig. 1. Experimental transfer characteristics of BC (squares) and TC (triangles) pentacene TFTs, measured in vacuum at $V_{ds} = -1$ V ($L = 100$ μm, $W = 200$ μm, $d_{ox} = 150$ nm).

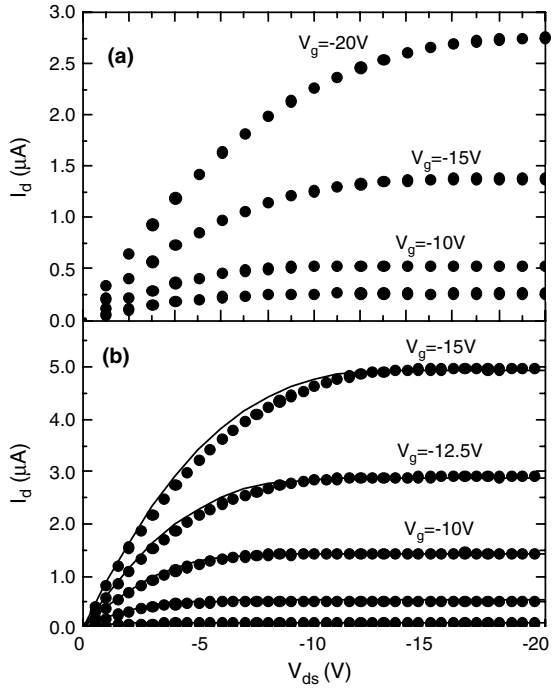


Fig. 2. Experimental (symbols) output characteristics of BC (a) and TC (b) pentacene TFTs, measured at $T = 300$ K and different gate voltages ($L = 100$ μm, $W = 200$ μm, $d_{ox} = 60$ nm). Also shown are the simulated output characteristics of TC pentacene TFT (b, solid lines).

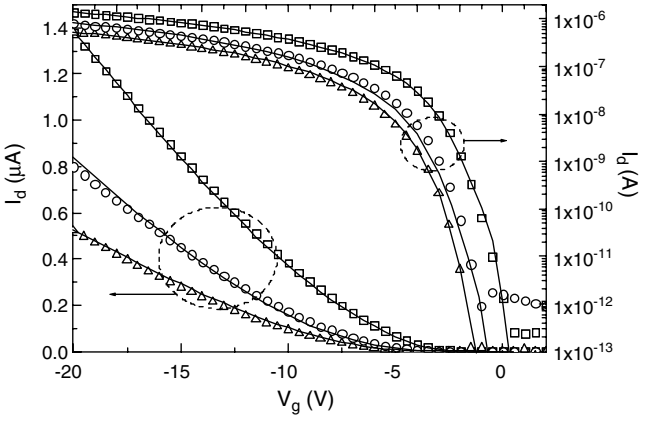


Fig. 3. Simulated (lines) and experimental (symbols) transfer characteristics (measured in vacuum at $V_{ds} = -1$ V), of as-fabricated TC pentacene TFTs for three different temperatures: 300 K (squares), 240 K (circles), 205 K (triangles) ($L = 100$ μm, $W = 200$ μm, $d_{ox} = 60$ nm).

from the slope of the linear portion of the transfer characteristics, monotonically increases with temperature.

In order to analyze the electrical properties we assume that the density of localized states, DOS, is uniformly distributed within the active layer, an approximation that has been shown to be very successful in describing the electrical characteristics of polycrystalline silicon TFTs [10]. The use of a uniform DOS approximation is particularly attractive, since strongly simplify the device analysis. Therefore, we applied the method developed in Ref. [11] to extract the DOS from the analysis of the sheet conductance, $G$,

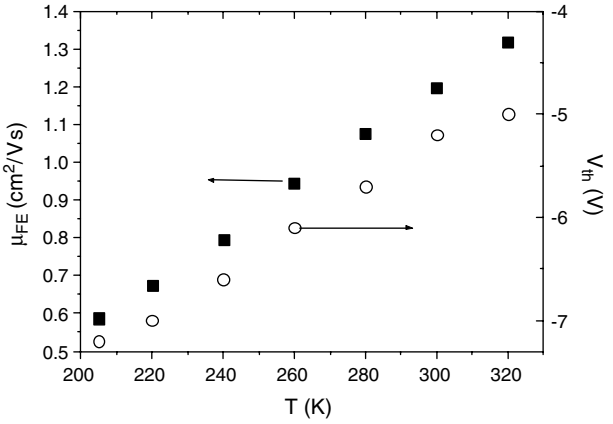


Fig. 4. Field effect mobility, $\mu_{FE}$, and threshold voltage, $V_{th}$, vs temperature of TC pentacene TFT.

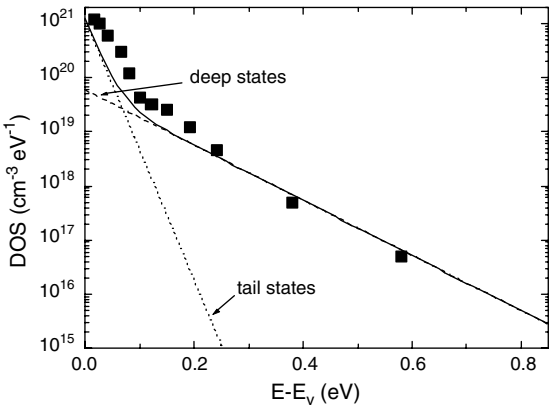


Fig. 6. Density of localized states calculated by the 'temperature method' (symbols). Solid line represents the approximated DOS used for the numerical simulations.

at different temperatures (temperature method). In particular, to eliminate the $G$–temperature dependence upon mobility, we used the normalized sheet conductance $G' = G\mu_{FE}(300\ \mathrm{K})/\mu_{FE}(T)$, where $G = I_d/V_{ds}$ is the sheet conductance which can be deduced from the $I_d$–$V_g$ characteristics measured at low $V_{ds}$, while $\mu_{FE}(T)$ is the temperature dependent field effect-mobility, shown in Fig. 4. According to the above mentioned method, the activation energy, $\Delta E$, of the $dG'/dV_g$ is equal to $\Delta E_o - q\Psi_s$, where $\Delta E_o$ is the energy difference between the Fermi level and the valence band edge at flat-band and $\Psi_s$ is the surface potential. In Fig. 5 a plot of $\Delta E$ vs $V_g - V_{fb}$ is shown, where $V_{fb} = 0.1$ V is the flat-band voltage determined according to the method proposed in Ref. [12]. As can be seen, the activation energy falls rapidly from $\Delta E = 0.6$ eV (for flat-band condition) down to few meV for $|V_g - V_{fb}| > 6$ V. The DOS, $N(E)$, can be deduced by calculating the surface electric field, $d\Psi_s/dx$, using the data for the activation energy shown in Fig. 5 and then using the following equation [11]:

$$N(E_F + \Psi_s) = \frac{\varepsilon_{Si}}{2q}\frac{\partial^2}{\partial \Psi_s^2}\left(\left.\frac{d\Psi}{dx}\right|_{x=0}\right)^2. \quad (1)$$

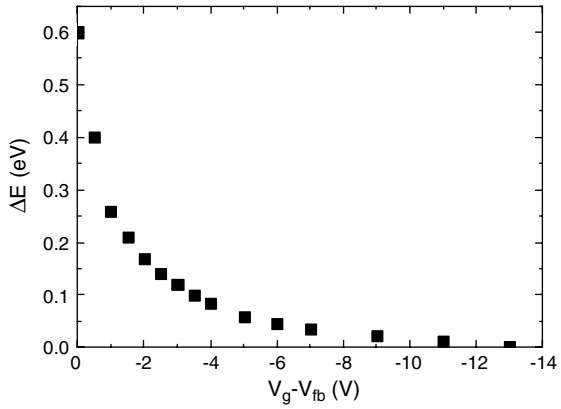


Fig. 5. Plot of the activation energy, $\Delta E$, derived from the Arrhenius plot of $dG'/dV_g$, vs $V_g - V_{fb}$. The flat band voltage, $V_{fb} = 0.1$ was calculated by the method reported in Ref. [12].

The calculated DOS (shown in Fig. 6) can be reasonably approximated by the sum of two exponential tails (see solid lines in Fig. 6):

$$N(E) = N_t \cdot e^{\frac{E-E_F}{E_t}} + N_d \cdot e^{\frac{E-E_F}{E_d}}, \quad (2)$$

where $N_t = 1.2 \times 10^{21}\ \mathrm{cm}^{-3}\ \mathrm{eV}^{-1}$, $E_t = 17$ meV, $N_d = 6 \times 10^{19}\ \mathrm{cm}^{-3}\ \mathrm{eV}^{-1}$ and $E_d = 85$ meV.

This approximated DOS was used in the 2D numerical device analysis program DESSIS, using conventional drift–diffusion transport model, to simulate the transfer and output characteristics at different temperatures. In DESSIS the energy distribution of the semiconductor density of states is modeled by four exponential terms, two of which located in the lower half of the bandgap (donor-like) and two in the upper half of the bandgap (acceptor-like). The energy distribution was taken symmetrical with respect to the midgap. The hole band mobility, $\mu_h$, was assumed constant for fixed temperature and variations with the transverse electric field were considered negligible. The dependence of $\mu_h$ with temperature was taken proportional to the temperature variations of field-effect mobility, considering $\mu_h = 1.58\ \mathrm{cm}^2/\mathrm{V\ s}$ at room temperature. The effective density of valence band states, $N_v$, was estimated assuming a square root energy distribution at the top of the valence band density of states and the effective mass for holes has taken to be equal to one electron mass [3]. Such an approximation is valid considering a relatively wide valence (HOMO) band of pentacene (~1 eV), as suggested by UPS spectra and bandstructure calculations [13].

As can be seen from Figs. 2 and 3, the transfer and output characteristics are very well reproduced in the temperature range considered. These results confirm that the model based on the spatially uniform DOS and conventional drift–diffusion transport model can be effectively used to analyze the transfer characteristics of pentacene TFTs and that the DOS, obtained from the 'temperature method', is quite accurate.

## 4. Conclusions

We have fabricated high quality pentacene OTFTs in top and bottom contact configurations with field effect mobility higher than 1 $cm^2/V$ s. The transfer characteristics of top contact, measured at different temperature, were analyzed using the 'temperature method', under the assumption of a spatially uniform distribution of localized states. As in the case of amorphous silicon, the calculated DOS can be approximated by the sum of two exponential tails (tail states and deep states). It should be pointed out that the calculated DOS is an effective DOS, including the contributions of the in-grain and grain boundary defects as well as of the dielectric/pentacene interface defects. Finally, by using the extracted DOS, it was possible to perfectly reproduce the pentacene-based TFT characteristics, using the 2D numerical device analysis program DESSIS, assuming drift–diffusion transport model.

## Acknowledgement

This work was supported by the project MICROPOLIS, under the program FIRB funded by Italian ministry of Education University and Research (MIUR).

## References

[1] G. Horowitz, J. Mater. Res. 19 (2004) 1946.
[2] C.D. Dimitrakopoulos, P.R.L. Malenfant, Adv. Mater. 14 (2002) 1999.
[3] A.R. Volkel, R.A. Street, D. Knipp, Phys. Rev. B 66 (2002) 195336.
[4] Y.S. Yang, S.H. Kim, J. Lee, H.Y. Chu, L. Do, H. Lee, J. Oh, T. Zyung, M.K. Ryu, M.S. Jang, Appl. Phys. Lett. 80 (2002) 1595.
[5] C.R. Kagan, A. Afzali, T.O. Graham, Appl. Phys. Lett. 86 (2005) 193505.
[6] F. De Angelis, T. Toccoli, A. Pallaoro, N. Coppedè, L. Mariucci, G. Fortunato, S. Iannotta, Synth. Met. 146 (2004) 291.
[7] F. De Angelis, S. Cipolloni, L. Mariucci, G. Fortunato, Appl. Phys. Lett. 86 (2005) 203505.
[8] C.D. Sheraw, L. Zhou, J.R. Huang, D.J. Gundlach, T.N. Jackson, M.G. Kane, I.G. Hill, M.S. Hammond, J. Campi, B.K. Greening, J. Francl, J. West, Appl. Phys. Lett. 80 (2002) 1088.
[9] H. Klauk, M. Halik, U. Zschieschang, F. Eder, G. Schimd, C. Dehm, Appl. Phys. Lett. 82 (2003) 4275.
[10] L. Mariucci, F. Giacometti, A. Pecora, F. Massussi, G. Fortunato, M. Valdinoci, L. Colalongo, Electron. Lett. 34 (1998) 924.
[11] G. Fortunato, D.B. Meakin, P. Migliorato, P.G. Le Comber, Philos. Mag. B 57 (1988) 573.
[12] R.L. Weisfield, D.A. Anderson, Philos. Mag. B 44 (1981) 83.
[13] G.A. de Wijs, C.C. Mattheus, R.A. de Groot, T.T.M. Palstra, Synth. Met. 139 (2003) 109.